RSC Advances

PAPER

Glycerol hydrogenolysis to propanediols over supported Pd–Re catalysts

Yuming Li,[a] Huimin Liu,[a] Lan Ma[ab] and Dehua He*[a]

Supported Pd–Re bi-component catalysts were prepared by an impregnation method and employed in a glycerol hydrogenolysis reaction. The addition of Re into a Pd catalyst increased the conversion of glycerol and the selectivities to propanediols. The catalysts were characterized by N_2 adsorption–desorption, XRD, CO chemisorption, TPR and NH_3-TPD techniques. The results showed that the addition of Re changed the reduction behaviors of the Pd and Re components, indicating that Pd and Re might have an interaction. Re could increase the ability of the catalysts for the activation of a C–O bond and further promote the activity of Pd in glycerol hydrogenolysis. At the same time, the addition of Re also increased the acidity of the Pd–Re catalysts. Pd–Re supported on acidic oxides showed a tendency of decreasing selectivities to 1,2-propanediol, while Pd–Re catalysts with basic oxides as supports could increase the conversion of glycerol, but maintain the selectivities to 1,2-propanediol.

Introduction

In recent years, the increased consumption of fossil fuels and the serious pollution of the environment has encouraged people to find new ways to solve the problem of energy supply. There are forecasts that a 50% growth in energy supply will be needed by 2025.[1,2] Biodiesel is a new kind of diesel fuel which is environment friendly, cheap and reproducible. It has gained much attention from the petrochemical industry for new resource production and its market is still growing. Biodiesel is produced by the transesterification of fatty acid esters or vegetable oils, with methanol or ethanol. In this process, glycerol, that accounts for nearly 10 wt% of production, is cumulated as a by-product.[3,4] For this reason, glycerol can not be considered as a high value-added chemical, but an over-produced feedstock. Traditionally, glycerol is used in cosmetics and to produce glycerin trinitrate. How to change this abundant glycerol into more valuable downstream products is a problem for chemists and manufacturers.[5,6]

From glycerol hydrogenolysis, 1,2-propanediol (1,2-PD) and 1,3-propanediol (1,3-PD) can be formed and they are high value-added products. 1,2-PD can be used to produce polyester resins, cosmetics, antifreeze and so on. 1,3-PD can be used in polyester fibers, medicines and so on.[7,8]

The main catalysts for this reaction can be divided into two types. One type are non-noble metal based catalysts and the other one is noble metal based catalysts. For the non-noble metals, Cu and Ni have been widely investigated. Cu and Ni catalysts can obtain 70–85% of glycerol conversion and 50–99% of selectivity to 1,2-PD.[9,10] Pd, Ru and Pt are active components used as noble metal catalysts. Musolino et al.[11] used Pd/Fe_2O_3 at 200 °C and 2-propanol as a H_2 donor and obtained results of 100% of glycerol conversion and 94% of selectivity to 1,2-PD after an 18 h reaction. Jiang et al.[12] used Ru–Cu bimetallic catalysts and found 100% of glycerol conversion and 86.4% of selectivity to 1,2-PD after 10 h reaction at 230 °C. Hamzah et al.[13] prepared $Ru/bentonite–TiO_2$ as a catalyst, over which the reaction was carried out at 150 °C, 2 MPa of H_2 for 7 h; 69.6% of glycerol conversion and 80.6% of selectivity to 1,2-PD were obtained. Additionally, Re has also been used in glycerol hydrogenolysis recently. In our previous study,[14] Re was added into a Ru catalyst and the Ru–Re catalyst was used in glycerol hydrogenolysis at 160 °C and 8 MPa H_2 for 8 h. A yield of 51.7% of glycerol conversion and 44.8% of selectivity to 1,2-PD were obtained for $Ru–Re/SiO_2$. These results were much higher than those of the Ru catalyst itself. In other papers, Pt–Re,[15] Rh–Re[16] and Ir–Re[17] were also investigated. In this literature, the researchers reported that the addition of Re into other metals could increase the activities of the active components in glycerol hydrogenolysis.

In recent research on glycerol hydrogenolysis, Pd has not been investigated significantly.[11] Compared with Ru and Pt, the activity of Pd is not as high as the Ru and Pt components. In our previous study, the addition of Re could increase the activity of Ru catalysts.[14] However, Ru based catalysts also tended to promote the over-hydrogenolysis or degradation of glycerol, which resulted in the formation of a large amount of CH_4 as a by-product. Compared with the Ru component, Pd, as an active component, produces little CH_4 in glycerol hydrogenolysis. In

[a]Innovative Catalysis Program, Key Lab of Organic Optoelectronics & Molecular Engineering of Ministry of Education, Department of Chemistry, Tsinghua University, Beijing 100084, China. E-mail: hedeh@mail.tsinghua.edu.cn; Fax: +86-10-62773346; Tel: +86-10-62773346

[b]Institute of Chemical Defence, Beijing 102205, China

this study, we report the catalytic behaviors of Pd catalysts and the feature of the products distribution. Furthermore, the bi-component Pd–Re catalysts were also investigated in glycerol hydrogenolysis. The addition of Re could increase the catalytic activity of Pd catalysts. For Pd–Re/SBA-15, as the content of Re increased, the conversion of glycerol also increased; at the same time, the selectivity to 1,2-PD decreased. The relationship between the catalytic performance and the physico–chemical properties of the Pd–Re catalysts were also examined.

Experiments

Materials

P123 ($EO_{20}PO_{70}EO_{20}$, $M_w = 5800$) was purchased from Sigma-Aldrich. $PdCl_2$ and $Pd(NO_3)_2$ were brought from Shenyang Nonferrous Metal Research Institute. $HReO_4$ (75–80% solution) was purchased from Alfa Aesar.

Al_2O_3 was purchased from the Aluminum Corporation of China. CNTs were obtained from the Department of Chemical Engineering, Tsinghua University. TiO_2, MgO, La_2O_3 and CeO_2 and the other materials (all samples were analytical reagents) were purchased from the Beijing Chemical Reagent Company.

Catalyst preparation

SBA-15 was prepared by using the method reported in the literature.[18–20] P123, as a template, was dissolved in a HCl aqueous solution (2 mol L^{-1}) with strong stirring, at 35 °C. After the solution became transparent, tetraethoxysilane (TEOS) was added to the solution and stirring continued for another 20 h at 35 °C. 0.017P123 : 40H_2O : 4.78HCl : 1TEOS was the molar ratio of the initial gel. Then, the solution was sealed and kept statically in an oven at 80 °C for 24 h. After that, the mixture was cooled to room temperature and washed with deionized water, until the filtrate became neutral. After being dried at 40 °C, the solid was calcined at 500 °C for 6 h in the air.

The CNTs were pretreated with a 5 mol L^{-1} HNO_3 solution at 110 °C for 5 h. After that, they were filtered and washed with deionized water, until the filtrate became neutral. The resultant sample was dried in the air at 110 °C for 12 h. The other supports were used as received.

The Pd/support catalysts were prepared with the impregnation method. $PdCl_2$ was dissolved in an HCl aqueous solution first. Then, the support was added into a certain amount of this $PdCl_2$ solution. After being impregnated, with stirring for 10 h in room temperature, the solvent was removed by evaporation. The catalyst was dried at 110 °C for 10 h, and reduced with H_2 at 250 °C for 2 h. The theoretical content of the Pd was 5 wt%. The catalysts were denoted as 5Pd/support.

5Pd–xRe/support catalysts were also prepared by the method of impregnation. A $HReO_4$ aqueous solution was mixed with the $PdCl_2$ aqueous solution, firstly. The other procedures were the same as the preparation of the Pd/support catalysts. (The 5Pd–xRe/support means a 5 wt% of Pd and an x wt% of Re.)

Other bi-component catalysts, such as 5Pd–5Ag/SBA-15, 5Pd–5Fe/SBA-15 and 5Pd–5Mn/SBA-15 catalysts, were all prepared by the method, the same as the Pd–Re/SBA-15 catalysts. The

contents of the Pd, Ag, Fe, and Mn were 5 wt%. The precursors for Fe and Mn were $Fe(NO_3)_3$ and $Mn(NO_3)_2$. For the preparation of Pd–Ag/SBA-15, $Pd(NO_3)_2$ and $AgNO_3$ were used as the precursors.

Hydrogenolysis of glycerol

The hydrogenolysis of glycerol was carried out in a stainless steel autoclave (100 mL) equipped with a magnetic stirrer. 10 mL of a 40 wt% of glycerol aqueous solution and 0.15 g Pd catalyst were added to the autoclave. After the autoclave was sealed, H_2 was used to replace the air inside it. The autoclave was tested for leaks, and then heated to 200 °C at 0.1 MPa H_2. Finally the pressure of the H_2 in the autoclave was increased to 8 MPa H_2 and the reaction started, with stirring. The reaction continued for 18 h. After reaction, the autoclave was cooled below 5 °C and then decompressed. The gas phase products were collected and analyzed with a gas chromatograph (Beijing Weisifu-GC 6890) equipped with a TDX-01 (4 mm × 2 m) column and a thermal conductivity detector (TCD). The gas phase products were quantified with an external standard method. The liquid phase products were separated from the catalyst with centrifugation and analyzed with a gas chromatograph (Lunan-SP 6890) equipped with a PEG-20M (0.22 mm × 30 m) column and a flame ionization detector (FID). An internal standard method was used to quantify the liquid products.

The conversion of glycerol and the selectivity to the products were calculated based on following equations.

$$\text{Conversion} (\%) = \frac{\text{Sum of } C \text{ mol of all products}}{\text{Added glycerol before reaction } (C \text{ mol})} \times 100\%$$

$$\text{Selectivity} (\%) = \frac{C \text{ mol of each product}}{\text{Sum of } C \text{ mol of all products}} \times 100\%$$

Catalyst characterization

The texture properties of all the samples were characterized by N_2 adsorption–desorption, with a Micromeritics ASAP 2010C analyzer. The BET and BJH methods were used for the analysis. Each sample was firstly treated at 300 °C in N_2 for 1.5 h and degassed at 300 °C for 4 h, then measured by N_2 adsorption at −197 °C.

Powder X-ray diffraction (XRD), which was used to characterize the phase structures of the 5Pd–xRe/SBA-15 and others, was carried out on a Rigaku D/max 2500. The instrument was powered at 40 kV and 200 mA. For wide angle XRD, the scan step was 10° min^{-1} with CuKα radiation ($\lambda = 0.1542$ nm). For small angle XRD, the scan step was changed to 1° min^{-1}. The particle sizes of the Pd were calculated by the Scherrer equation.

The H_2 temperature programmed reduction (H_2-TPR) measurements were carried out in a chemical adsorption instrument (Quantachrome CHEM-300). A sample, of 0.1 g, was firstly treated in pure Ar gas (99.999%) at 250 °C for 2 h and then cooled down to room temperature. The TPR was firstly performed by maintaining the sample at 30 °C in 5% of H_2–Ar gas

(20 mL min^{-1}) for 20 min. (Step I) Then, the sample was heated from 30 °C to 500 °C at a heating rate of 15 °C min^{-1}. (Step II) A cool trap, prepared by liquid nitrogen and isopropanol, was used before the TCD detector, to prevent the effect of water during the TPR measurements.

In the H$_2$-TPR experiments, the sample was pre-treated in pure Ar gas before starting the TPR. Therefore, when switching the sample from pure Ar gas to the H$_2$–Ar gas to start the TPR, some residual Ar gas remained in the sample tube. So, the residual Ar gas in the sample tube would cause a response in the baseline of the TCD detector, which showed as a peak at the beginning of the TPR profile at 30 °C. On the other hand, the PdO could be reduced, even at 30 °C. This also brought a H$_2$ consumption peak at 30 °C at the beginning of the TPR profile, after changing the gas from Ar into H$_2$–Ar. For these reasons, a blank TPR (with SBA-15 only in the tube) was measured as a comparative test, to confirm the disturbance of changing the gas from Ar into H$_2$–Ar.

The dispersion of Pd was measured with a CO pulsed chemical adsorption method. The experiment was carried out in a chemical adsorption instrument Quantachrome CHEM-300. The catalyst sample (0.1 g) was firstly reduced in pure H$_2$ gas for 2 h at 250 °C. Then, the sample was cooled in 99.999% He gas (the trace amount of oxygen in He gas was removed by a deoxidizer) to 30 °C. The CO chemisorption was performed by pulsing a certain amount of CO into the sample tube at 30 °C. The dispersion of Pd was obtained by calculating the adsorption amount of the CO in the Pd sample.

The NH$_3$-TPD profiles of the catalysts were measured in a chemical adsorption instrument (Quantachrome CHEM-300) with a quadrupole mass-spectrometer detector (DM200M Gas Analyzer). In a typical operation, 0.1 g of the sample was pre-treated at 250 °C for 2 h in flowing He gas (99.999%) and then cooled. After the temperature reached 100 °C, the flowing gas was changed into 1% NH$_3$–He gas and swept through the sample for 0.5 h, for the adsorption. After sweeping again with pure He gas at 100 °C for 0.5 h to remove the physical adsorption of NH$_3$, the sample was heated in flowing He gas (20 mL min^{-1}) from 100 °C to 500 °C at the heating rate of 15 °C min^{-1} and the mass signals were recorded. The NH$_3$ desorption signal was identified with $m/z = 16$ (NH$_2$). The desorption amount of NH$_3$ was calculated by integrating the NH$_3$-TPD peak areas, which were calibrated by the mass signal of the standard NH$_3$–He gas.

The morphologies of the catalysts were characterized by high-resolution transmission electron microscopy (HR-TEM). A JEM-2010 JEOL, equipped with an energy dispersive spectrometer (EDS) was used. The catalysts were all reduced at 250 °C with H$_2$ for 2 h before the characterization.

The X-ray photoelectron spectroscopy (XPS) was recorded on a PHI Quantera SXM of ULVAC-PHI Inc. The binding energy of the sample was calibrated with the C 1s peak (284.6 eV). The 5Pd–5Re/SBA-15 catalyst was reduced at 250 °C with H$_2$ for 2 h, before the characterization.

Results and discussion

The catalytic performance of bi-component Pd–M/SBA-15 catalysts and the effect of Re addition on glycerol hydrogenolysis

The catalytic performances of the different bi-component catalysts with Pd and another metal components (Ag or Fe, Mn, Re) in the glycerol hydrogenolysis are shown in Table 1. From the results, the addition of Ag, Fe or Mn had little effect on the performance of the Pd/SBA-15 in this reaction. The conversions of glycerol for these three catalysts were all lower than 2%, but the selectivities to 1,2-PD were all higher than that of the Pd/SBA-15 itself. The addition of Re had the most obvious effect among these catalysts. The conversion of glycerol increased from 1.5% to 40.7% when Re was added. Moreover, the addition of Re to Pd/SBA-15 also showed an effect on the selectivity to 1,3-PD. The selectivities to 1,3-PD and 1-propanol (1-PO) increased from 4.4% and 14.6% to 8.2% and 24.6%, respectively. However, the selectivity to 1,2-PD decreased from 72.2% to 59.9%. In addition, for these mono-component Pd and bi-component Pd–M catalysts, CH$_4$ was nearly not detected. It is suggested that the addition of Re into the Pd catalyst might bring some interaction between the Pd and Re, and could affect the glycerol hydrogenolysis significantly. In order to investigate the performance of the addition of Re into the Pd catalysts, a further investigation was undertaken.

The texture properties of 5Pd–xRe/SBA-15 catalysts and effect of Re amount on catalytic activity

The pore structures and surface areas of all the 5Pd–xRe/SBA-15 catalysts were analyzed by a low temperature nitrogen

Table 1 Performance of 5Pd–5M/SBA-15 in glycerol hydrogenolysis[a]

Cat.	Conv. (%)	Select. (%)							
		CH$_4$	MeOH	EtOH	EG	1-PO	2-PO	1,2-PD	1,3-PD
5Pd/SBA-15	1.5	0.0	0.7	2.1	5.3	14.6	0.7	72.2	4.4
5Pd–5Ag/SBA-15	0.9	0.0	0.7	1.2	8.6	8.2	1.1	79.2	1.1
5Pd–5Fe/SBA-15	1.7	0.0	1.1	1.2	5.1	8.3	0.4	83.2	0.7
5Pd–5Mn/SBA-15	1.8	0.0	0.9	1.0	9.7	2.9	0.2	84.6	0.7
5Pd–5Re/SBA-15	40.7	2.0	0.1	1.3	1.8	24.6	2.1	59.9	8.2

[a] *Reaction conditions*: 10 mL 40 wt% glycerol solution, 0.15 g 5% Pd catalyst, 200 °C, 8 MPa H$_2$, 18 h, 700 rpm. MeOH: methanol, EtOH: ethanol, EG: ethylene glycol, PO: propanol.
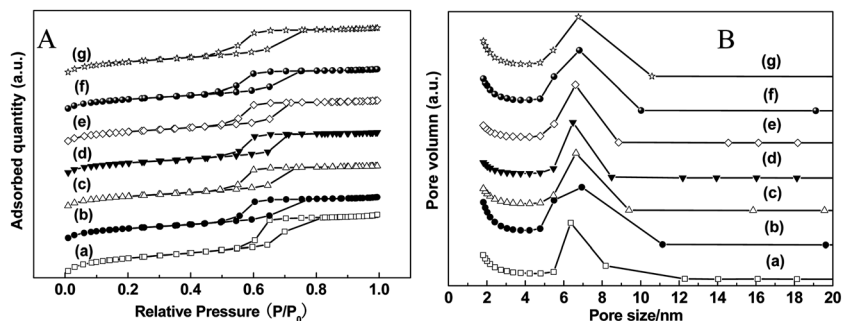
Fig. 1 N₂ adsorption–desorption isotherms (A) and pore size distributions (B) of 5Pd−xRe/SBA-15 (a): SBA-15, (b): 5Pd/SBA-15, (c): 5Pd−1Re/SBA-15, (d): 5Pd−3Re/SBA-15, (e): 5Pd−5Re/SBA-15, (f): 5Pd−10Re/SBA-15, and (g): 5Re/SBA-15.

Table 2 Texture properties of 5Pd−xRe/SBA-15

	S_{BET} (m² g⁻¹)	V (cm³ g⁻¹)	D_{BJH} (nm)
SBA-15	856.1	0.71	5.70
5Pd/SBA-15	670.5	0.53	5.39
5Pd−1Re/SBA-15	648.9	0.52	5.37
5Pd−3Re/SBA-15	662.0	0.52	5.31
5Pd−5Re/SBA-15	618.2	0.53	5.36
5Pd−10Re/SBA-15	589.6	0.59	5.36
5Re/SBA-15	704.9	0.59	5.38

adsorption technique. The N₂ adsorption–desorption isotherms are shown in Fig. 1. These results indicated that the SBA-15 and all 5Pd−xRe/SBA-15 catalysts had hysteresis loops and showed type IV isotherms, revealing that all the catalysts maintained a mesoporous structure after the reduction. In the meantime, it also showed that after the reduction, the N₂ adsorption–desorption isotherms were quite similar, except that the hysteresis loops moved to lower P/P_0, compared with the SBA-15 itself. Table 2 shows the BET surface area, the pore volume and the average pore size of the 5Pd−xRe/SBA-15 samples. From the results, SBA-15 had the largest surface area (856.1 m² g⁻¹). After the reduction, the surface areas of all the 5Pd−xRe/SBA-15 catalysts became smaller. The 5Pd−10Re/SBA-15 had the smallest surface area (589.6 m² g⁻¹). It can be seen from the results that the surface area of 5Pd/SBA-15 was smaller than that of 5Re/SBA-15. For the pore volume and average pore size, SBA-

15 had the largest pore volume (0.71 cm³ g⁻¹) and average pore size (5.70 nm); 5Pd−xRe/SBA-15 catalysts all had similar pore volume (0.5–0.6 cm³ g⁻¹) and average pore size (5.3–5.4 nm). Fig. 1 shows the pore size distributions of the 5Pd−xRe/SBA-15 catalysts. From the results, it revealed that after impregnation and reduction, the 5Pd−xRe/SBA-15 catalysts all had a wider pore size distribution than SBA-15. This may be because the addition of Pd and Re to the SBA-15 would decrease the steric regularity of the SBA-15.

The catalytic performances of the 5Pd−xRe/SBA-15 catalysts with the addition of different Re content in the glycerol hydrogenolysis are shown in Table 3. From the results, a mono-component Pd or Re catalyst showed very low conversions of glycerol (1.5% and 3.1%, respectively). After adding Re into the 5Pd/SBA-15, the conversions of glycerol increased. As the content of Re increased from 1% to 10%, the conversions of glycerol increased from 10.2% to 45.1%, and the selectivities to 1,3-PD and 1-PO also increased from 5.2% and 5.8% to about 8% and 20%, respectively. But the selectivity to 1,2-PD decreased from 77.5% to 60%. The total selectivities to CH₄, methanol and ethanol were lower than 6% for each catalyst. It is suggested that in the mono-component Pd or bi-component Pd–Re catalysts, the tendency of degradation of glycerol was very weak. From the above results, it indicated that the addition of Re can influence the Pd catalysts performance in this reaction. To compare the activities of the Pd–Re and Pd catalysts more clearly, the TOF (turnover frequency) of the 5Pd/SBA-15 and 5Pd−5Re/SBA-15 were calculated, with the conversion of glycerol being near 10%. For the 5Pd/SBA-15, the TOF was 1.7 h⁻¹. After

Table 3 Performance of 5Pd−xRe/SBA-15 in glycerol hydrogenolysis[a]

Cat.	Conv. (%)	Select. (%)							
		CH₄	MeOH	EtOH	EG	1-PO	2-PO	1,2-PD	1,3-PD
5Pd/SBA-15	1.5	0.0	0.7	2.1	5.3	14.6	0.7	72.2	4.4
5Pd−1Re/SBA-15	10.2	5.0	0.3	0.7	5.0	5.8	0.6	77.5	5.2
5Pd−3Re/SBA-15	19.9	2.6	0.2	0.8	3.7	9.3	0.8	74.4	8.3
5Pd−5Re/SBA-15	40.7	2.0	0.1	1.3	1.8	24.6	2.1	59.9	8.2
5Pd−10Re/SBA-15	45.1	3.0	0.1	1.6	3.0	21.7	1.6	60.4	8.6
5Re/SBA-15	3.1	0.0	0.4	1.4	1.7	38.7	1.5	49.6	6.7

[a] Reaction conditions: 10 mL 40 wt% glycerol solution, 0.15 g 5% Pd catalyst, 200 °C, 8 MPa H₂, 18 h, 700 rpm.

the addition of Re, the TOF of 5Pd–5Re/SBA-15 increased to 22.7 h^{-1}. The addition of Re therefore increased the activity of Pd catalysts in glycerol hydrogenolysis.

The structure of 5Pd–xRe/SBA-15 catalysts and the interaction between Pd and Re

The XRD patterns of 5Pd–xRe/SBA-15 are shown in Fig. 2. For the small angle XRD, all the 5Pd–xRe/SBA-15 catalysts had a diffraction peak at $2\theta = 1°$, which meant that they all maintained the well-ordered mesoporous structure of SBA-15. From the wide angle XRD patterns of 5Pd/SBA-15 and 5Pd–xRe/SBA-15, the diffraction peaks of Pd(111) at $2\theta = 40°$, Pd(200) at $2\theta = 46°$ and Pd(220) at $2\theta = 68°$ were observed. These results are consistent with references.[21-23] For the wide angle XRD pattern of the 5Re/SBA-15, a very weak peak at $2\theta = 43°$, which belonged to Re, could be found. However, for 5Pd–xRe/SBA-15, the peaks belonging to Re could not be observed. This might be due to the dispersion of the Re component on the support[16] or ReO_4^- formation from the interaction of Re and the support.[24] Some of the Re might interact with the Pd, and an alloy or bimetallic cluster might be formed.[25,26] This perhaps also led to the unobserved Re peaks.

From the XRD characterization results of 5Pd/SBA-15, 5Pd–1Re/SBA-15 and 5Pd–3Re/SBA-15, it can be seen that the intensities of the Pd peaks of those samples were similar. As the content of Re increased to 5% or 10%, the Pd peak intensity of 5Pd–5Re/SBA-15 or 5Pd–10Re/SBA-15 became a little higher.

The Pd dispersions of 5Pd–xRe/SBA-15 were measured by the CO chemisorption method, as shown in Table 4. For the 5Pd/SBA-15, the dispersion of Pd was 17.3%. The addition of Re into the Pd/SBA-15 catalyst made the dispersion of Pd on 5Pd–xRe/SBA-15 decrease somewhat, but with no great difference. The Pd dispersion of 5Pd–1Re/SBA-15 was 14.3%. As the added amount of Re increased from 1% to 10%, the dispersion of Pd on the 5Pd–xRe/SBA-15 (x = 3–10) caused no evident change.

Fig. 3 and 4 show the TEM images of the 5Pd/SBA-15 and 5Pd–5Re/SBA-15 catalysts. From Fig. 3, the Pd particle size distribution of the 5Pd/SBA-15 catalyst had a broad range, of 3–21 nm. With EDX analysis, the Pd element was confirmed on the surface of the 5Pd/SBA-15. The mean particle size of the Pd in the 5Pd/SBA-15 was 11.1 nm. For the 5Pd–5Re/SBA-15 (Fig. 4), it was clearly shown that the noble metal particles were homogeneously distributed on the support. With the EDX analysis of the metal particles, both the Pd and Re elements were observed, indicating that the two metals might be combined together on the surface of the support. For these particles, the average particle size was 5.1 nm, with the size distribution between 3–7 nm. At the same time, it could be seen that the particles grew along the channels of the SBA-15, which made the particles grow with a rod-like shape.

The TPR profiles of 5Pd–xRe/SBA-15 are shown in Fig. 5. In Step I of the TPR experiments (the sample was kept in flowing 5% H$_2$/Ar at 30 °C for 20 min), all the TPR profiles revealed a reduction peak. For the blank test (with SBA-15 only), this peak (blank peak) in the TPR profile belonged to the TCD signal of the residual Ar, due to changing the carrier gas (Ar) into 5% H$_2$–Ar, while for the other samples (5Pd/SBA-15, 5Pd–xRe/SBA-15 and 5Re/SBA-15), the reduction peaks at 30 °C belonged to the sum of the blank and the H$_2$ consumption. For Step II of the TPR experiments, the profiles of 5Pd/SBA-15 and 5Pd–xRe/SBA-15 showed negative peaks at 100 °C, due to the decomposition
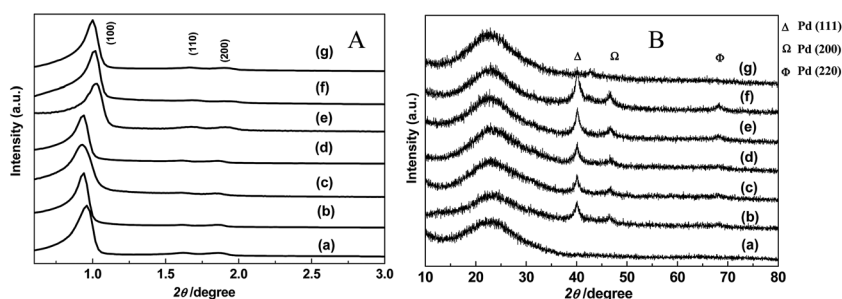
Fig. 2 Small angle (A) and wide angle (B) XRD patterns of 5Pd–xRe/SBA-15 (a): SBA-15, (b): 5Pd/SBA-15, (c): 5Pd–1Re/SBA-15, (d): 5Pd–3Re/SBA-15, (e): 5Pd–5Re/SBA-15, (f): 5Pd–10Re/SBA-15, and (g): 5Re/SBA-15.

Table 4 Dispersions of Pd on 5Pd–xRe/SBA-15 and H$_2$ consumption in TPR[a]

	Dispersion[a] (%)	H$_2$ consumption of Step I (mmol)	H$_2$ consumption of Step II (mmol)	Total H$_2$ consumption (mmol)
5Pd/SBA-15	17.3	0.025	0.013	0.037
5Pd–1Re/SBA-15	14.3	0.035	0.016	0.051
5Pd–3Re/SBA-15	14.1	0.054	0.030	0.085
5Pd–5Re/SBA-15	13.7	0.076	0.055	0.132
5Pd–10Re/SBA-15	13.3	0.092	0.126	0.217
5Re/SBA-15	—	−0.001	0.097	0.096

[a] Obtained from CO chemisorption.
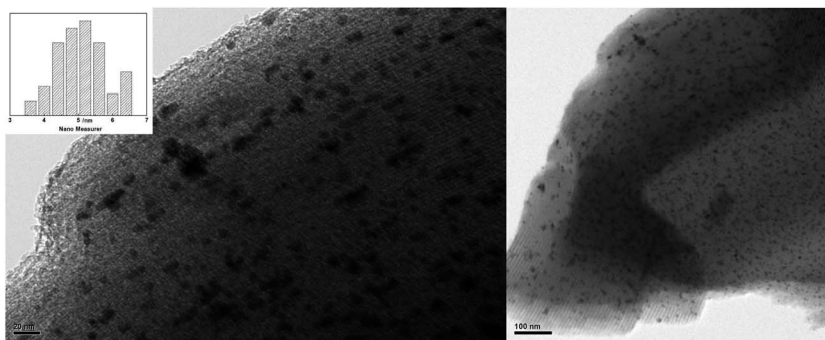
Fig. 3 The TEM image of the Pd–Re/SBA-15 catalyst after reduction at 250 °C.
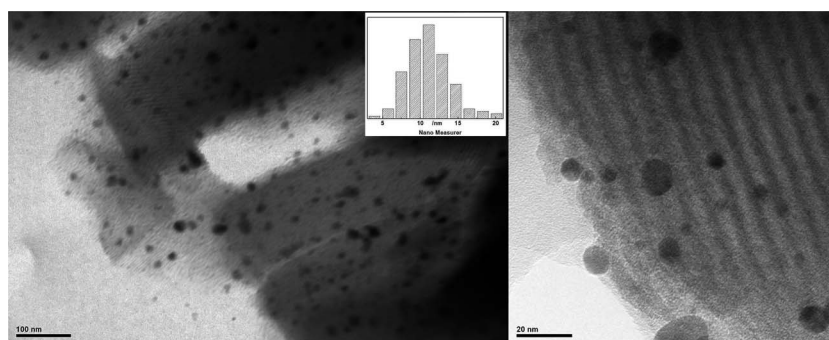
Fig. 4 The TEM image of the Pd/SBA-15 catalyst after reduction at 250 °C.
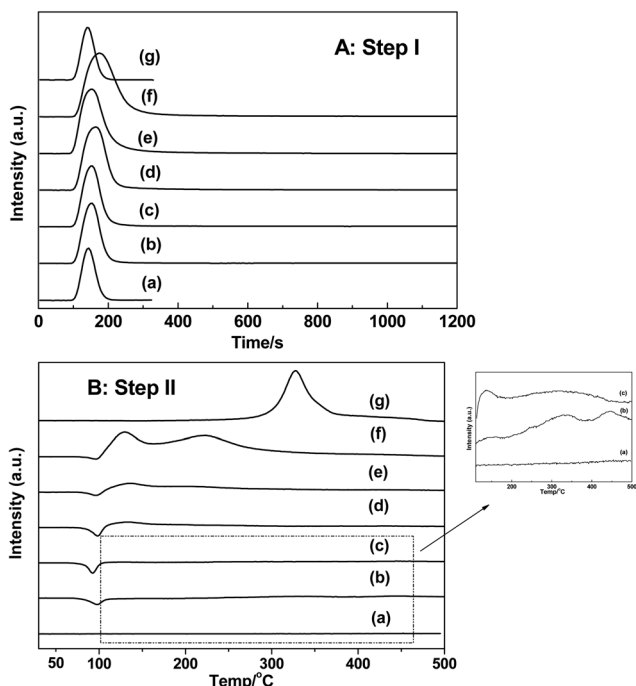
Fig. 5 H$_2$-TPR profiles (maintained at 30 °C) of 5Pd–xRe/SBA-15 and blank tests (a): SBA-15, (b): 5Pd/SBA-15, (c): 5Pd–1Re/SBA-15, (d): 5Pd–3Re/SBA-15, (e): 5Pd–5Re/SBA-15, (f): 5Pd–10Re/SBA-15, and (g): 5Re/SBA-15. A, Step I: the samples were maintained at 30 °C for 20 min in flowing 5% H$_2$/Ar B, Step II: then the samples were heated in flowing 5% H$_2$/Ar from 30 °C to 500 °C at 15 °C min^{-1}.

of PdH. For the 5Pd/SBA-15, Pd oxide could be reduced at nearly 30 °C (Fig. 5b). During the reduction process of PdO, the reduced Pd could form a PdH species.[27,28] At about 100 °C, the PdH species would decompose and release H$_2$, forming a negative peak.[27,28] Re oxide on the 5Re/SBA-15 could be reduced at 330 °C (Fig. 5f). It has been reported that Re oxides alone were hardly reduced at low temperatures, and easily sublimated at high temperatures. For 5Pd–xRe/SBA-15, the TPR profiles were different from the 5Pd/SBA-15 and 5Re/SBA-15. For the 5Pd–3Re/SBA-15 and 5Pd–5Re/SBA-15 (Fig. 5d and e), the intensities of the peaks at 30 °C in the TPR profiles were higher than that of the 5Pd/SBA-15. For the TPR profile of the 5Pd–5Re/SBA-15, besides the reduction peak at 30 °C, a new reduction peak at 130 °C appeared. These results suggested that some of the Re oxide on the 5Pd–xRe/SBA-15 might be reduced at lower temperatures, compared with the 5Re/SBA-15. As the amount of Re increased to 10%, the reduction peaks in the TPR profile of the 5Pd–10Re/SBA-15 were observed at about 30 °C, 130 °C and 220 °C. For all the 5Pd–xRe/SBA-15, no reduction peak was found when the temperature was higher than 250 °C. This was quite similar to another report.[28] The consumption amounts of H$_2$ during the TPR were calculated and the results are provided in Table 4. From the results, it can be seen that as the content of Re increased, the consumption amounts of H$_2$ in both Step I and Step II all increased for 5Pd–xRe/SBA-15, compared with 5Pd/SBA-15. Combined with the TPR profiles, it is suggested that the addition of Re could have an interaction with Pd, making the reduction temperature of Re lower.
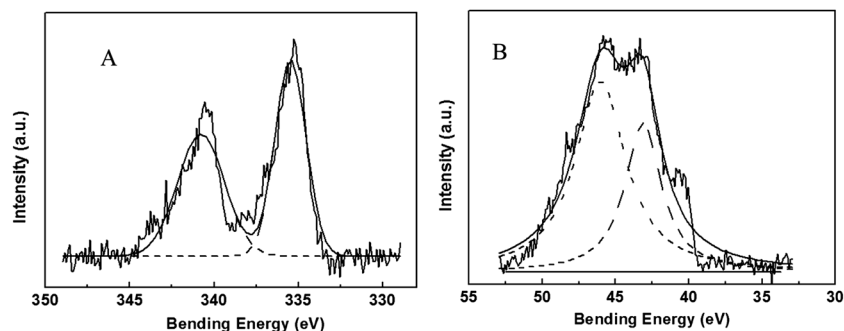
Fig. 6 XPS spectrum of Pd 3d and Re 4f after reduction at 250 °C A: Pd 3d in 5Pd–5Re/SBA-15 B: Re 4f in 5Pd–5Re/SBA-15.

The chemical species of Pd and Re in the Pd–Re catalyst, after reduction, were evaluated by XPS. Fig. 6 shows the results of the XPS of the 5Pd–5Re/SBA-15. All the XPS spectra of Pd and Re were calibrated in energy by the C 1s signal at 284.6 eV. For the Pd XPS spectrum (Fig. 6A), the binding energies (BE values) of the Pd $3d_{3/2}$ and $3d_{5/2}$ core levels were 340.78 eV and 335.47 eV, respectively. These results all had a shift to higher BE values, compared with other references.[29,30] For the XPS spectrum of Re (Fig. 6B), values of 46.02 eV and 43.11 eV for the Re^{4+} and Re^{6+} oxidation states were observed, respectively. Compared with other references,[31,32] the BE values of Re became a little lower for the 5Pd–5Re/SBA-15 catalyst. Combined with the XPS analysis of Pd, it indicated that the there should be an electron transfer, from Pd to Re in this catalyst, which suggested that Pd and Re had an interaction.[33,34]

For the Pd–Re catalysts, from the TPR and XPS results, it could be supposed that the addition of Re into Pd might cause the interaction between the Pd and Re components, and could change the reduction behaviors and the electronic states of the Pd and Re oxide. It was possible that part of the Pd and Re interacted to form a Pd–Re alloy[25] or a bi-component cluster.[26] Pallassana et al.[35] used non-local density functional theory (DFT) calculations and found that in the hydrogenolysis of acetic acid, the C–OH bond may be in favor of activating on the Re surface rather than on the Pd surface. The reason may be that the barrier of C–OH bond activation on the Re surface was lower than on the Pd surface. But for the hydrogenation process, Pd was much better than Re.[35,36] This may also occur in glycerol hydrogenolysis with Pd–Re catalysts. Re could activate the C–O bond and Pd could help the intermediate react with the H_2. The catalytic efficiency of the Pd–Re catalysts may, therefore, become higher.

Fig. 7 shows the NH_3-TPD profiles of the 5Pd–xRe/SBA-15 catalysts. For the SBA-15, no NH_3 desorption could be detected in the TPD. This indicated that SBA-15 had no acidity. For 5Pd/SBA-15, the TPD profile showed an NH_3 desorption peak at 200 °C. For 5Re/SBA-15, NH_3 desorption peaks were detected at 160 °C and 240 °C, which meant it had two kinds of acidic sites with different acid strengths. The acid strength of 5Re/SBA-15 was stronger than that of the 5Pd/SBA-15. Additionally, the amount of acid for the 5Re/SBA-15 was also larger than that for the 5Pd/SBA-15. Table 5 shows the acid amounts of the 5Pd–xRe/SBA-15 catalysts, which were calculated from the desorption peaks of the NH_3-TPD. From the 5Pd/SBA-15, the acid
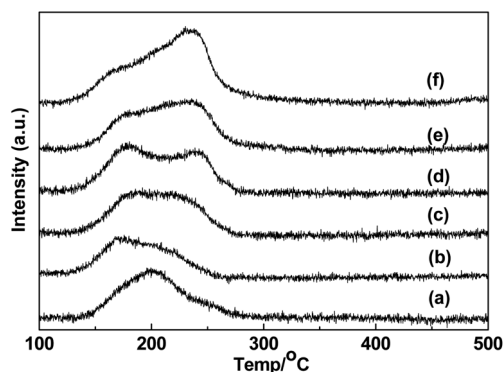
Fig. 7 NH_3-TPD profiles of 5Pd–xRe/SBA-15 (a): 5Pd/SBA-15, (b): 5Pd–1Re/SBA-15, (c): 5Pd–3Re/SBA-15, (d): 5Pd–5Re/SBA-15, (e): 5Pd–10Re/SBA-15, and (f): 5Re/SBA-15.

amount was 108.2 μmol g^{-1}, and the acid amount of Re/SBA-15 was 245.2 μmol g^{-1}, which was twice as much as the 5Pd/SBA-15. From the NH_3-TPD profile of the 5Pd–1Re/SBA-15, it clearly showed that an NH_3 desorption peak at 160 °C appeared, which meant the addition of Re into 5Pd/SBA-15 could affect the acidity of the catalysts. As shown in Fig. 7, as the contents of Re increased, the NH_3-TPD profiles of the 5Pd–xRe/SBA-15 catalysts became increasingly similar to that of the 5Re/SBA-15. When the content of Re increased to 3% and 5%, the NH_3 desorption peaks at both 160 °C and 240 °C appeared. The NH_3-TPD profile of the 5Pd–10Re/SBA-15 showed a strong NH_3 desorption peak at 240 °C, and the strength of the peak was stronger than that of the other 5Pd–xRe/SBA-15 catalysts. From Table 5, it can also been seen that the addition of Re from 1% to 10% would

Table 5 Acid amounts of 5Pd–xRe/SBA-15[a]

	NH_3^{a} μmol g^{-1}
5Pd/SBA-15	108.2
5Pd–1Re/SBA-15	129.0
5Pd–3Re/SBA-15	135.2
5Pd–5Re/SBA-15	174.6
5Pd–10Re/SBA-15	210.6
5Re/SBA-15	245.2

[a] Obtained from NH_3-TPD.

increase the acid amount of the catalysts from 108.2 μmol g^{-1} to 210.6 μmol g^{-1}.

The acidity of the catalysts may influence the catalytic activity and the distribution of the products. Fig. 8 shows the relationship of the acid amounts and the glycerol conversion. From the results, it clearly shows that increasing the Re content led to the increase of acidity of the 5Pd–xRe/SBA-15. Also, as the acidity of the 5Pd–xRe/SBA-15 increased, the conversion of glycerol increased. For the mono-component Re catalyst (5Re/SBA-15), the conversion of glycerol was very low, because of the absence of Pd, which was the active site for hydrogenation. For the 5Pd–xRe/SBA-15, when the addition of Re was excessive (5Pd–5Re/SBA-15 and 5Pd–10Re/SBA-15), the acid amount significantly increased. However, from the reaction results (Table 3), it can be seen that the selectivity to 1,2-PD decreased and the selectivity to 1-PO increased over the 5Pd–5Re/SBA-15 and 5Pd–10Re/SBA-15 catalysts. The selectivity to 1,3-PD increased somewhat as the acid amount increased. From the results mentioned above, the change in the acid amount might cause the change of the conversion of glycerol and the distribution of the products.

From other references regarding the addition of Re,[37–39] some mechanistic paths were also discussed. Chia et al.[37] used NH$_3$-TPD characterization and DFT calculations for Rh–Re catalysts in the hydrogenolysis of polyols and cyclic ethers. They found that the bi-component Rh–Re catalysts were acidic. The DFT results suggested that the hydroxyl group in the Re would make the intermediates more stable. Tomishige et al.[38,39] found that hydride and proton were easily formed and a C–O bond neighbouring a CH$_2$OH group could be catalyzed by Ir–Re, or Rh–Re catalysts. For Pd–Re catalysts in the present study, combined with the references mentioned above, ReO$_x$ might supply the hydroxyl group that could change the acid properties of the catalysts. This kind of hydroxyl group and the interaction of Pd–Re might be favourable for catalyzing the C–O bond of glycerol and accelerating the dehydration of glycerol to intermediates. Acetol or 3-hydroxypropanal might be formed as intermediates of the dehydration of glycerol. In the present study, the 5Pd–5Re/SBA-15 and 5Pd/SBA-15 catalysts were used
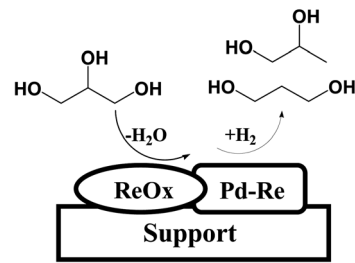
Scheme 1 Working mechanism of the Pd-Re/SBA-15 catalyst.

for the dehydration of glycerol into acetol. The formation rate of acetol, over 5Pd–5Re/SBA-15 (4.2 mmol g$_{cat}^{-1}$ h^{-1}), was nearly 4 times that over 5Pd/SBA-15 (1.1 mmol g$_{cat}^{-1}$ h^{-1}). From these results, the addition of Re could surely increase the dehydration process in glycerol hydrogenolysis. After dehydration, these intermediates would undergo a further hydrogenation reaction and 1,2-PD, 1,3-PD and other produces would formed.

Combined with the reaction and characterization results mentioned above, we propose a working mechanism of the Pd–Re/SBA-15 catalyst in the reaction of glycerol hydrogenolysis, as shown in Scheme 1. That is, Pd and Re might interact, to form bimetallic clusters. With the help of ReO$_x$, the processes of the dehydration of glycerol into intermediates and the hydrogenation of the intermediates into propanediols becomes easier, compared with the mono-component Pd catalysts.

The support effect on catalytic performance of Pd–Re catalysts in glycerol hydrogenolysis

Pd and Pd–Re catalysts with different supports (CNTs, Al$_2$O$_3$, TiO$_2$, MgO, La$_2$O$_3$ and CeO$_2$) were also prepared by an impregnation method and employed in glycerol hydrogenolysis. The reaction results are shown in Table 6. The activities of the mono-component Pd catalysts with different supports were not high. The conversion of glycerol over 5Pd/CNTs was the highest among all the mono-component Pd catalysts (12.7%), and the others were all lower than 10%. For 5Pd/Al$_2$O$_3$, the conversion was the lowest, at only 3.3%. The selectivities to 1,2-PD over the mono-component Pd catalysts were all higher than 70%. At the same time, the selectivities to 1-PO over the Pd catalysts with acidic oxide supports (such as Al$_2$O$_3$) were higher than those over Pd supported on basic oxides (MgO, La$_2$O$_3$ and CeO$_2$). After the addition of Re to the Pd catalysts, the performance of the Pd–Re catalysts with different supports was changed substantially compared with the mono-component Pd catalysts. The addition of Re increased the activities of the Pd catalysts supported on different supports. These results are in accordance with Pd–Re/SBA-15.

On the other hand, from Table 6, the performance of the Pd–Re catalysts supported on acid oxides (or neutral oxides) and basic oxides still had some differences. The addition of Re into 5Pd/CNTs, for example, the conversion of glycerol over 5Pd–5Re/CNTs increased from 12.7% to 49.6%. However, the selectivities to 1,2-PD and ethylene glycol (EG) decreased from 71.0% and 4.8% to 52.5% and 1.7%, respectively. Meanwhile, the
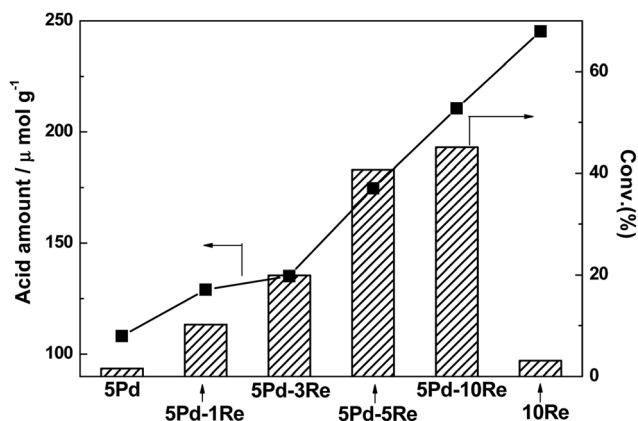
Fig. 8 Relationship of glycerol conversion, acid amount and Re content of the 5Pd–xRe/SBA-15 catalysts.

Table 6 Performance of Pd–Re catalysts supported on different supports in glycerol hydrogenolysis[a]

Cat.	Conv. (%)	Selec. (%)							
		CH_4	MeOH	EtOH	EG	1-PO	2-PO	1,2-PD	1,3-PD
5Pd–5Re/CNTs	49.6	1.9	0.1	1.9	1.7	30.0	3.7	52.5	8.2
5Pd/CNTs	12.7	0.0	1.4	0.3	4.8	12.9	1.8	71.0	7.9
5Pd–5Re/Al_2O_3	23.6	1.5	0.1	1.0	1.2	26.6	1.5	54.5	13.6
5Pd/Al_2O_3	3.3	0.0	0.3	0.9	5.6	19.3	0.8	63.3	9.9
5Pd–5Re/TiO_2	20.9	3.5	0.1	1.2	4.7	14.0	0.6	70.1	5.7
5Pd/TiO_2	4.9	4.5	0.5	1.0	8.8	2.4	0.2	80.8	1.8
5Pd–5Re/MgO	35.1	2.4	0.8	1.0	3.9	6.0	0.9	81.7	3.3
5Pd/MgO	9.4	4.5	0.5	1.6	8.8	1.7	0.2	81.3	1.5
5Pd–5Re/La_2O_3	52.9	0.4	1.2	0.6	2.7	2.7	1.0	89.3	2.1
5Pd/La_2O_3	8.0	0.0	2.1	2.3	10.4	1.7	0.6	83.0	0.0
5Pd–5Re/CeO_2	15.9	1.1	1.4	0.3	4.8	1.7	0.3	89.2	1.1
5Pd/CeO_2	6.4	0.0	1.4	0.6	5.4	2.3	0.6	88.1	1.7

[a] *Reaction conditions*: 10 mL 40 wt% glycerol solution, 0.15 g 5% Pd catalyst, 200 °C, 8 MPa H_2, 18 h, 700 rpm.

selectivity to 1-PO increased from 12.9% to 30.0%, and the selectivity to 1,3-PD increased a little (from 7.9% to 8.2%). The same phenomena were also observed over 5Pd–5Re/SBA-15 (in Table 3), 5Pd–5Re/Al_2O_3 and 5Pd–5Re/TiO_2. In addition, over 5Pd–5Re/MgO, the conversion of glycerol increased from 9.4% to 35.1% compared with 5Pd/MgO. Unlike the 5Pd–5Re/CNTs, the selectivity to 1,2-PD over 5Pd–5Re/MgO was 81.7%, which did not decrease compared with 5Pd/MgO. The distribution of products changed little over the 5Pd/MgO and 5Pd–5Re/MgO catalysts. The results of 5Pd–5Re/La_2O_3 and 5Pd–5Re/CeO_2 also showed similar behaviours, like the 5Pd–5Re/MgO. These results suggested that the acidic oxides could influence the acidity of the Pd–Re catalysts and result in the further hydrogenolysis of the products, while the basic oxides could limit further reaction of the products and maintain the selectivity to 1,2-PD.

Conclusions

Pd mono-component catalysts showed activities in glycerol hydrogenolysis, but the activities were not high. After the addition of Re, the activities of the Pd catalysts increased significantly. From the TPR of 5Pd–xRe/SBA-15, it was shown that the reduction temperature of Re was decreased and that Re and Pd might interact. The interaction between Pd and Re was also found from the XPS of 5Pd–5Re/SBA-15. Moreover, the addition amount of Re also influenced the catalytic activities and the distribution of the products. The acid amounts of 5Pd–xRe/SBA-15 increased with increasing Re loading, and this could result in the further reaction of propanediols and increase the formation of 1-propanol.

Acknowledgements

Notes and references

1 A. Ragauskas, C. Williams and B. Davison, *Science*, 2006, **311**, 484.
2 D. Liang, J. Gao, H. Sun, P. Chen, Z. Hou and X. Zheng, *Appl. Catal., B*, 2011, **106**, 423.
3 M. Musolino, L. Scarpino, F. Mauriello and R. Pietropaolo, *ChemSusChem*, 2011, **4**, 1143.
4 L. Li, T. Korányi, B. Sels and P. Pescarmona, *Green Chem.*, 2012, **14**, 1611.
5 D. Alonso, S. Wettstein and J. Dumesic, *Chem. Soc. Rev.*, 2012, **41**, 8075.
6 J. Ma, J. Song, H. Liu, J. Liu, Z. Zhang, T. Jiang, H. Fan and B. Han, *Green Chem.*, 2012, **14**, 1743.
7 T. Miyazawa, S. Koso, K. Kunimori and K. Tomishige, *Appl. Catal., A*, 2007, **329**, 30.
8 K. Wang, M. Hawley and S. DeAthos, *Ind. Eng. Chem. Res.*, 2003, **42**, 2913.
9 S. Xia, R. Nie, X. Lu, L. Wang, P. Chen and Z. Hou, *J. Catal.*, 2012, **296**, 1.
10 J. Hu, X. Liu, B. Wang, Y. Pei, M. Qiao and K. Fan, *Chin. J. Catal.*, 2012, **33**, 1266.
11 M. Musolino, L. Scarpino, F. Mauriello and R. Pietropaolo, *Green Chem.*, 2009, **11**, 1511.
12 T. Jiang, Y. Zhou, S. Liang, H. Liu and B. Han, *Green Chem.*, 2009, **11**, 1000.
13 N. Hamzah, N. Nordin, A. Nadzri, Y. Nik, M. Kassim and M. Yarmo, *Appl. Catal., A*, 2012, **419–420**, 133.
14 L. Ma and D. He, *Top. Catal.*, 2009, **52**, 834.
15 O. Daniel, A. DeLaRiva, E. Kunkes, A. Datye, J. Dumesic and R. Davis, *ChemCatChem*, 2010, **2**, 1107.
16 Y. Shinmi, S. Koso, T. Kubota, Y. Nakagawa and K. Tomishige, *Appl. Catal., B*, 2010, **94**, 318.
17 Y. Nakagawa, X. Ning, Y. Amada and K. Tomishige, *Appl. Catal., A*, 2012, **433–434**, 128.
18 W. Zhou and D. He, *Chem. Commun.*, 2008, 5839.
19 W. Zhou and D. He, *Green Chem.*, 2009, **11**, 1146.

20 C. Zhang, W. Zhou and S. Liu, *J. Phys. Chem. B*, 2005, **109**, 24319.

21 B. Xue, P. Chen, Q. Hong, J. Lin and K. Tan, *J. Mater. Chem.*, 2001, **11**, 2378.

22 L. Shao, B. Zhang, W. Zhang, D. Teschner, F. Schlol and D. Su, *Chem.–Eur. J.*, 2012, **18**, 14962.

23 X. Liang, C. Liu and P. Kuai, *Green Chem.*, 2008, **10**, 1318.

24 W. Phongsawat, B. Netiworaruksa, K. Suriye, S. Dokjampa, P. Praserthdam and J. Panpranot, *J. Nat. Gas Chem.*, 2012, **21**, 158.

25 Y. Sato, K. Terada, S. Hasegawa, T. Miyao and S. Naito, *Appl. Catal., A*, 2005, **296**, 80.

26 W. Juszczyk and Z. Karpinski, *Appl. Catal., A*, 2001, **206**, 67.

27 N. Babu, N. Lingaiah, R. Gopinath, P. Reddy and P. Prasad, *J. Phys. Chem. C*, 2007, **111**, 6447.

28 R. Pérez-Hernández, A. Avendaño, E. Rubio and V. Rodríguez-Lugo, *Top. Catal.*, 2011, **54**, 572.

29 B. Mao, R. Chang, S. Lee, S. Axnanda, E. Crumlin, M. E. Grass, S. Wang, S. Vajda and Z. Liu, *J. Chem. Phys.*, 2013, **138**, 214304.

30 M. V. Castegnaro, A. S. Kilian, I. M. Baibich, M. Alves and J. Morais, *Langmuir*, 2013, **29**, 7125.

31 F. John, F. William, E. Peter and D. Kenneth, *Handbook of X-ray Photoelectron Spectroscopy*, Minnesota, USA, 1995.

32 T. Tsoncheva, S. Vankova, O. Bozhkov and D. Mehandjiev, *Can. J. Chem.*, 2007, **85**, 118.

33 R. Campbell, J. Rodriguez and D. Goodman, *Phys. Rev. B: Condens. Matter*, 1992, **46**, 7077.

34 H. Kima, H. Parka, T. Kima, K. Jeonga, H. Chaea, S. Jeonga, C. Leeb and C. Kima, *Catal. Today*, 2012, **185**, 73.

35 V. Pallassana and M. Neurock, *J. Catal.*, 2002, **209**, 289.

36 Y. Takeda, Y. Nakagawa and K. Tomishige, *Catal. Sci. Technol.*, 2012, **2**, 2221.

37 M. Chia, Y. Torres, D. Hibbitts, Q. Tan, H. Pham, A. Datye, M. Neurock, R. Davis and J. Dumesic, *J. Am. Chem. Soc.*, 2011, **133**, 12675.

38 S. Koso, Y. Nakagawa and K. Tomishige, *J. Catal.*, 2011, **280**, 221.

39 Y. Amadaa, Y. Shinmi, S. Kosoa, T. Kubot, Y. Nakagawaa and K. Tomishige, *Appl. Catal., B*, 2011, **105**, 117.